

****FULL TITLE****
*ASP Conference Series, Vol. **VOLUME**, **YEAR OF PUBLICATION***
****NAMES OF EDITORS****

Stellar Abundances: Recent and Foreseeable Trends

Carlos Allende Prieto

University of Texas, Austin, TX 787512, USA

Abstract. The determination of chemical abundances from stellar spectra is considered a mature field of astrophysics. Digital spectra of stars are recorded and processed with standard techniques, much like samples in the biological sciences. Nevertheless, uncertainties typically exceed 20%, and are dominated by systematic errors. The first part of this paper addresses what is being done to reduce measurement errors; and what is not being done, but should be. The second part focuses in some of the most exciting applications of stellar spectroscopy in the arenas of galactic structure and evolution, the origin of the chemical elements, and cosmology.

1. Introduction

Stellar absorption lines, first discovered in the solar spectrum circa 1804, can be used to quantify the proportions of different chemical elements in stars. The strength of the lines depends on the abundance of absorbers, but also on the environment where the absorption takes place: the stellar atmosphere. The determination of chemical abundances requires an accurate knowledge of the physical conditions (e.g. temperature, density, radiation field) in the outer layers of the star. In other words, inferring chemical abundances from spectra is just a part of the problem of the physics of stellar atmospheres, and cannot be decoupled from it.

After Eddington, Milne, and others established the theoretical basis, the field of quantitative stellar spectroscopy has evolved over time to become almost an industry. Stellar abundances have shed light on the origin of the elements, the early universe, what the interior of the stars look like, or how galaxies form and evolve. As modeling is refined, so are the quality and reach of the observations, making possible to use stellar abundances to tackle new problems.

Nowadays, a small army of some 10^3 researchers are *professionally* dedicated to measure chemical abundances from stellar spectra in the entire world. Practitioners favor B-type stars on the warm side, and F- and G-type stars on the cool side. B-type stars can be observed at large distances, while the cooler F- and G-types live long, allowing us to study the past. Cooler stars have far more complex spectra, shaped by molecular absorption and dust.

In this paper, with no ambition of formally reviewing the field, I simply highlight recent accomplishments and tendencies, both in methods (Section 2.) and applications (§3.). The closing section is devoted to a personal (and surely biased) reflection on where the field is going, and where one wishes it would go.

2. Stellar abundances. How to?

Telescopes and spectrographs are used to obtain stellar spectra. The visible is the window of choice for abundance measurements, because of the high transparency of the Earth's atmosphere, limited line crowding, and simple continuum opacities (basically H and H⁻). The result of an observation is an account of the detected stellar photons properly ordered by energy. The next step is removing instrumental effects that distort the observed photon distribution.

The final stage consists in translating observed line strengths into chemical abundances. This step involves many simplifications and assumptions that allow us to build an approximate description of the physical conditions in the atmosphere of the star, given a small number of parameters (energy flux, surface gravity, and metal abundances¹) to be inferred from observations. Libraries of atmospheric models are computed by experts, and then widely disseminated (or not). The fact that one of the model parameters, the metal abundance, is what we seek, makes this a problem that needs to be treated iteratively. In the standard procedure, the equation of radiative transfer is solved to calculate the spectra predicted by the models, which are then compared to an observation to constrain the atmospheric parameters, and estimate the metal abundances. This information is then used to select a new model that will be used to refine the abundances, going on until convergence is achieved.

Two critical parts of this process are the model atmospheres and the calculation of the emergent spectrum from the models. Obtaining the right observations and performing a reliable analysis are other key elements involved.

2.1. Model atmospheres

The model atmospheres commonly used today are based on the concepts of radiative and hydrostatic equilibrium. These models are one-dimensional: all the relevant thermodynamical quantities depend only on height (plane-parallel geometry) or radius (spherical models). Models for late-type stars also assume local thermodynamical equilibrium (LTE), i.e. the source function is equal to the Planck law and therefore only depends on the local temperature.

Spectral lines are most useful for deriving chemical abundances, but line absorption also affects the energy balance in the outer layers of a star. Iron is by far the element that produces most of the observed lines. Metal line crowding in the blue and UV spectra of late-type stars contributes significantly to the total opacity, inducing extra warming in deep atmospheric layers and cooling in the outer regions. Line blanketing becomes milder for hot stars, but even then it is still quite significant. Hot star models that account for both departures from LTE and line blanketing (see Fig. 1) have only become available recently (Hubeny & Lanz 1995, Lanz & Hubeny 2003, Rauch 2003, Repolust, Puls, J. & Herrero 2004). For the most massive stars, especially when dealing with UV spectra, winds need to be considered (Pauldrach et al. 2001, Hillier 2003).

¹Hereafter quantified in a logarithmic scale relative to hydrogen and solar values:
 $[X/H] = \log \frac{N_X}{N_H} - \log \left(\frac{N_X}{N_H} \right)_{\odot}$, where N represents number density.

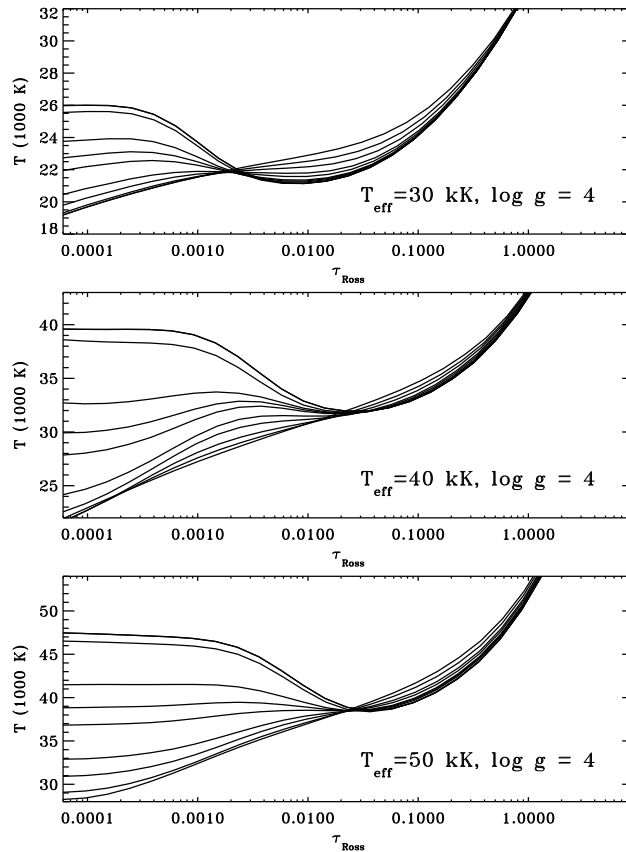


Figure 1. Temperature structure as a function of the Rosseland optical depth from the O-star grid of Lanz & Hubeny (2003). The different curves for any given T_{eff} correspond to metallicities from $2\times$ solar to zero. Departures from LTE are responsible for warming the outer layers of the more metal-poor models, where line cooling is not effective.

Models for late-type (F, G, and K-type) stars have been always based on the assumption that LTE holds. As stated above, line blanketing needs to be included. Unlike in more massive stars, convection develops in the envelopes of these stars to some degree. This is accounted for in the energy balance by a simplified treatment termed as mixing-length theory (Böhm-Vitense 1958). However, the impact of convection on the velocity fields at the surface of the star is usually ignored, i.e., hydrostatic equilibrium is still assumed. That this is a bad approximation is nowhere more evident than in a high-resolution image of the solar surface. Fig. 2 shows an area of the solar disk including a group of sunspots. The concentration of magnetic field in sunspots inhibits convection, which is responsible for the granular pattern apparent everywhere else, as evident in the section expanded in the right-hand panel of Fig. 2. The white areas correspond to bright granules: hot gas upflows. The dark lanes are the intergranules: cooler sinking gas. The temperature contrast in the solar photosphere ranges from several hundred to more than a thousand degrees, and the velocities reach a few

kilometers per second. Typical granules have angular sizes of about 1 arcsecond, or a couple thousand kilometers on the solar surface, and evolve on time scales of the order of 10–15 minutes.

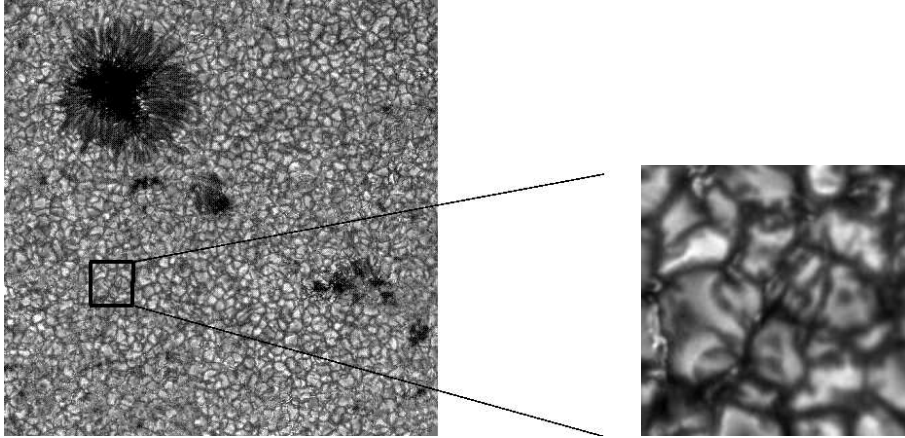


Figure 2. Image of the solar surface obtained with the Swedish 1-m Solar Telescope at La Palma. The continuum image (436.4 nm) shows a group of sunspots on August 22, 2003. Observations by O. Engvold, J. E. Wiik, and L. R. van der Voort (Inst. of Theoretical Astrophysics of Oslo University).

Hydrodynamical models that account for the temperature and velocity fields associated with convection, oscillations, and shocks in the solar atmosphere were pioneered more than two decades ago (e.g., Massaguer & Zahn 1980, Nordlund 1980, Hurlburt, Toomre & Massaguer 1984) and have now reached maturity (Stein & Nordlund 1998, Asplund et al. 2000a). Unlike classical model atmospheres, which have a constant temperature at any given depth, these models exhibit temperature and velocity inhomogeneities that resemble solar observations. Fig. 3 compares the temperature at a given depth in the photosphere for one-dimensional and three-dimensional models – compare with Fig. 2.

Classical static models predict perfectly symmetric spectral lines. The line profiles produced in hydrodynamical models are asymmetric and blue-shifted relative to their rest wavelengths as a result of the correlation between temperature and velocity fields – very much like the observed line profiles (Asplund et al. 2000a, Allende Prieto et al. 2002). In some cases, the strengths of spectral lines predicted by 3D and 1D models are significantly different. Occasionally, the ability of hydrodynamical models to reproduce closely the observed line shapes, allows us to identify blends that otherwise would go unnoticed.

A recent revision of the solar photospheric abundances of several light elements based on 3D models has arrived at the conclusion that both oxygen and carbon (but also Ne, Ar, Fe and Si) are significant less abundant, in some cases by as much as 40 %, than previously thought (Allende Prieto et al. 2001, 2002; Asplund et al. 2000b, 2004, 2005). The revised solar abundances show that hydrodynamics (and departures from LTE) are not mere refinements, but crucial ingredients. The updated abundances are in better agreement with other stars in the solar neighborhood, but they also ruin an earlier excellent agreement between helioseismic measurements and models of the solar interior (Bahcall et al.

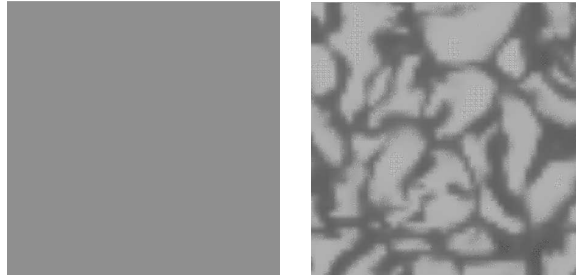


Figure 3. The gray scale indicates temperature at a given photospheric depth for a classical model atmosphere (left-hand panel), and in a snapshot of the hydrodynamical simulation of Asplund et al. (2000a).

2005a, Bahcall, Serenelli & Basu 2005c, Basu & Antia 2004, Antia & Basu 2005, Montalbán et al. 2004) – a conundrum that still needs a solution at the time of this writing (see Bahcall, Basu & Serenelli 2005b and Drake & Testa 2005 for possible light at the end of the tunnel, or Young & Arnett 2005 for a different source of light). Unfortunately, hydrodynamical models for stars other than the Sun are not widely available (and mostly non-existent). Moreover, the tools available to calculate spectra from time-dependent 3D hydrodynamical simulations are very limited, and unable, for example, to calculate emergent absolute fluxes with realistic (line and continuum) opacities over large spectral windows.

For stars with $T_{\text{eff}} < 4000$ K, molecules become very important both in the equation of state and in the radiative opacity (mainly H_2 , H_2O , CH_4 , CO , N_2 , NH_3 , FeH , CrH , TiO , and VO). In addition, for atmospheres cooler than $T_{\text{eff}} \sim 2500$ K, solid particles, such as silicates, which form clouds, are also an important source of opacity, with alkalis as the only atoms that still contribute significantly. The complicated opacities pose a challenge for modeling the coolest stars and brown dwarfs. Handling the formation and rainout of condensate clouds further complicates matters (e.g. Burrows, Sudarsky & Hubeny 2005, Tsuji 2005). Fig. 4 illustrates the change in the emergent flux between 700 K and 2100 K for models recently computed by Burrows et al. (2005) for a particular surface gravity, particle size, and cloud shape.

2.2. Spectrum formation

Although the radiation field needs to be continuously evaluated as model construction proceeds, the detailed calculation of the emergent spectrum for comparison with observations is usually performed afterwards. At this time, higher spectral resolution and a more accurate modeling of the line profiles becomes affordable as the equation of radiative transfer needs to be solved just a few times. It is also possible to estimate departures from LTE for trace species, assuming that the atmospheric structure (e.g. temperature and electron density) is given by an LTE model atmosphere previously calculated.

Reliable opacities, as we have discussed in §2.1., can be the limiting factor for obtaining realistic model atmospheres. For stars like the Sun, the optical and infrared continuum is shaped by bound-free and free-free absorption of H^- , a trace species nonetheless. In the UV window, however, atomic metal opacity

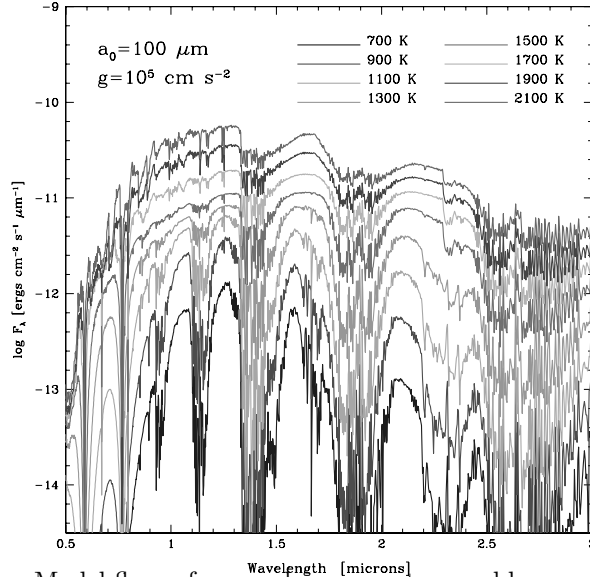


Figure 4. Model fluxes for very low mass stars and brown dwarfs (dividing line at $T_{\text{eff}} \sim 1700$ K) as they would be observed at a distance of 10 pc ($\log F \propto 2 \log R + 4 \log T_{\text{eff}}$, and the radii are adopted from Burrows et al. 1997). Adapted from Burrows, Sudarsky & Hubeny 2005.

(mainly due to Mg, Fe, and Al) becomes relevant, and even dominant at wavelengths below 250 nm. Quantum mechanical calculations in the context of the Opacity Project (OP) have provided accurate photoionization cross-sections for light elements (Seaton 2005), and an extension of the calculations to iron ions is ongoing within the Iron Project (IP; Nahar & Pradhan 2005). These data are (slowly) being incorporated in the calculation of theoretical spectra (Cowley & Bautista 2003, Allende Prieto et al. 2003a,b). Fig. 5 illustrates the impact of the bound-free metal absorption on the UV solar flux.

Another important aspect of the calculation of stellar spectra that has been recently improved is related to the absorption line coefficients. Improved calculations of cross-sections for line broadening by elastic hydrogen collisions have been presented by Paul Barklem and collaborators (see Barklem, Anstee, & O’Mara 1998, Barklem & Aspelund-Johansson 2005, and references therein). Improved absorption coefficients are also now available for Balmer lines (see, e.g., Barklem, Piskunov & O’Mara 2000, Barklem et al. 2002). The wings of the Balmer lines, formed in deep layers very close to LTE conditions, are very sensitive indicators of the effective temperature of a star (see Fig. 6). Interestingly enough, the mixing-length parameter for convection (α) needs to be reduced to about half a pressure scale height in order to get consistent temperatures from $H\alpha$ and $H\beta$ for solar like stars – the usual values inferred from standard solar models and multidimensional simulations of solar surface convection lead to $2 < \alpha < 2.1$ (Basu, Pinsonneault, & Bahcall 2000, Robinson et al. 2004). The new calculations of collisional broadening by atomic H have the largest impact for metal-poor stars, where gas pressure is higher than at solar metallicity, and have made it possible to reconcile effective temperatures inferred from colors and Balmer lines.

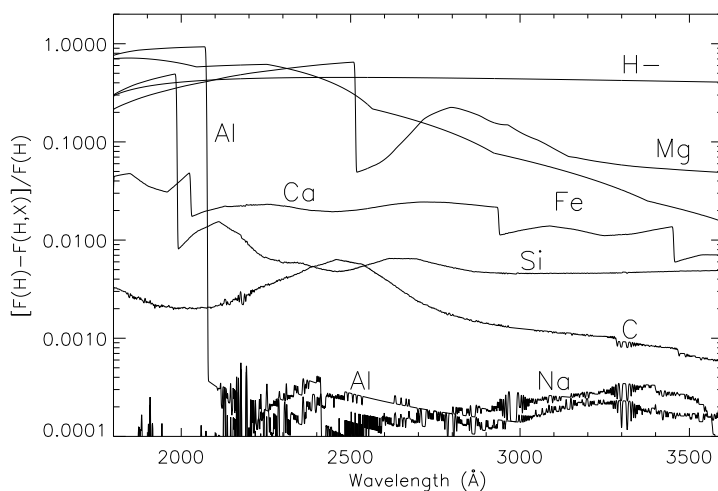


Figure 5. Relative changes in the emergent flux from a solar-like atmosphere when continuum opacity from H^- and several metals are added to the atomic hydrogen opacity (Allende Prieto, Hubeny & Lambert 2003b).

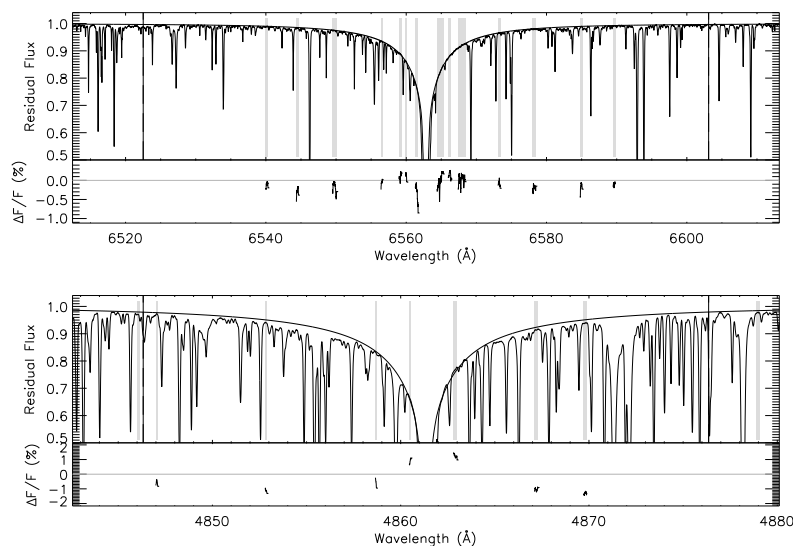


Figure 6. Fittings to the solar $H\alpha$ and $H\beta$ line profiles with a MARCS model (Gustafsson et al. 1975, 2003) for a mixing-length parameter $\alpha = l/H_p = 0.5$, the Stark broadening profiles of Stehlé (1994) and the hydrogen collision broadening profiles of Barklem, Piskunov, & O'Mara (2000). The grey areas indicate the spectral windows used to evaluate the goodness-of-fit. Adapted from Barklem et al. (2002).

The OP data base², TOPBASE, includes other useful data in addition to photoionization cross-sections: energy levels and transition probabilities, as well

²<http://vizier.u-strasbg.fr/topbase/home.html>

as tools to compute opacities and radiative forces. The computed energies for atomic levels are not very accurate, and although the opacities include corrections for the ground level of each species, they can be improved by using observed energies, readily available from other sources such as NIST³. OP and IP calculations assume LS coupling and neglect fine structure. For the line opacity, one commonly uses accurate observed line wavelengths. The most comprehensive atomic and molecular line lists have been compiled by Kurucz and collaborators (e.g., Kurucz 1993⁴). Kurucz has also calculated and compiled wavelengths and weights for hyperfine structure (*hfs*) and isotopic components.

A noteworthy development is the recent availability of laboratory determinations of atomic parameters (transition probabilities, hyperfine and isotopic splitting constants, and partition functions) for many rare-earth elements (e.g., Den Hartog et al. 2005; Lawler, Sneden & Cowan 2004; Den Hartog, Wickliffe & Lawler 2002; Lawler, Wyart & Blaise 2001). Fig. 7 shows how important it is to consider *hfs* when deriving abundances for elements like holmium.

While LTE constitutes a very useful approximation that makes the calculation of model atmospheres and spectra simple, it is often wrong. Calculations of Non-LTE line formation in LTE model atmospheres for trace species show abundant examples where line strengths interpreted with equilibrium (LTE) populations lead to large systematic errors in the inferred abundances. NLTE models for hot stars are now available, but the same cannot be said for late-type stars. This shortcoming is most likely the result of the extended belief that departures from LTE are small in late-type stars. In fact, recent calculations by Short & Hauschildt (2005) suggest that there are significant changes in the temperature structure of a solar model when LTE is relaxed. The same investigation also finds that a NLTE solar model matches the observed fluxes worse than an LTE model – a puzzling result which suggests that this is still an unfinished business.

A more extensive discussion of some of the issues mentioned in this and the previous section can be found in the reviews by Gustafsson & Jørgensen (1994), Allard et al. (1997), Asplund (2005), and Kirkpatrick (2005).

2.3. Observation and analysis

As modeling improves, so do some aspects of the data acquisition and analysis process. Quantities that have seen constant progress include the telescopes' diameter, the spectral coverage of spectrographs, and their multiplexing capabilities. However, a victim of the difficulty to couple large diameter telescopes with narrow slits, the resolving power has been neglected. Investigations of spectral line shapes, which are poorly matched by hydrostatic models and therefore nobody wants to see, have almost become *faux pas*.

Data reduction is done in most cases with packages such as IRAF or MIDAS. Pipelines for automatic reduction have been implemented for some facilities and large projects (e.g. Ritter & Washuettl 2004). For the most part, spectra are usually reduced interactively, which causes two problems: i) individual scientists, trying to move on as quickly as possible to the data analysis, do not dedicate the

³www.nist.gov

⁴<http://kurucz.harvard.edu>

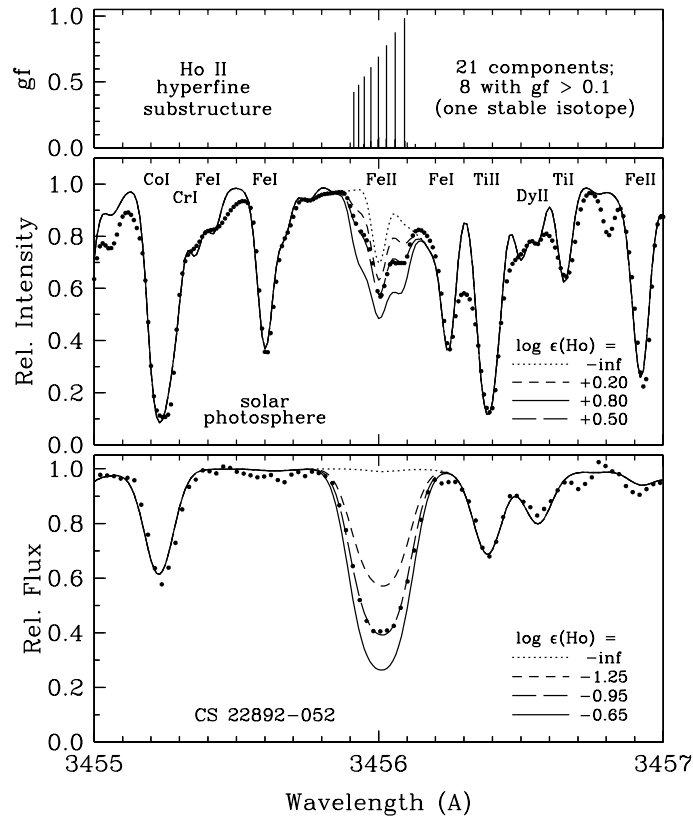


Figure 7. Ho II line at $\lambda 3456$. The lines in the top panel show the strengths and positions of the hyperfine splitting (hfs) components due to ^{165}Ho , the only stable isotope of holmium. The middle and lower panels show the spectrum of the Sun and the metal-poor star CS 22892-052 (see Section 3.1.), respectively. The impact of hfs in the line shape is quite dramatic, and Ho abundances inferred would be seriously in error if neglected. Adapted from Lawler, Sneden & Cowan (2005).

necessary amount of time to make sure the reduction is the best possible, and ii) the knowledge on data reduction is not encapsulated into software. A more efficient and better scheme would involve dedicated research on the data reduction process specific for an instrument, with the results subsequently captured into a pipeline. For example, Piskunov & Valenti (2002) have recently reminded us that going the extra mile pays off.

As data sets grow in size – more stars and more frequencies per star– it becomes necessary to automate not only the data reduction, but also the data analysis. For example, a spectroscopic analysis typically starts with a search for the best estimates of the atmospheric parameters: effective temperature, surface gravity and overall metal content. Such step is amenable to automation (Katz et al. 1998, Snider et al. 2001, Allende Prieto 2003, Erspamer & North 2003, Willemsen et al. 2005). Neural networks, genetic algorithms, self-organizing maps and many other kinds of optimization methods can help to relief the burden on the busy astronomer.

3. Stellar abundances. What for?

After some hard work, we get to the most exciting part: what can we do with the derived chemical abundances? A possible criterion to classify the applications of stellar abundances is whether or not they are based on the *golden rule*. The golden rule, a term introduced in this context by David Lambert, states that

The surface composition of a star reflects that of the interstellar medium at the time and location where the star formed.

As with any other good-looking law, the golden rule is often broken. But we will first see how to take advantage of those cases when it seems to hold.

3.1. When the golden rule applies

Only ^1H , ^2H , ^3He , ^4He , ^7Li and ^6Li were produced in significant amounts in the big bang, while heavier nuclei are mostly the result of stellar nucleosynthesis. When stars explode as supernovae, or lose mass from their envelopes by the action of stellar winds or thermal pulses on the asymptotic giant branch (AGB), the metals produced by stellar nucleosynthesis (explosive or not) enrich the interstellar medium. As low-mass stars have very long life spans (the hydrogen burning time scales $\propto M^{-5/2}$), if the golden rule applies, one can use stars of different ages to track the metal enrichment of the interstellar medium with time. An account of the state of this field is given in this volume by Yeshe Fenner, so I just briefly mention some recent observational developments that illustrate how stellar abundances can help to understand how galaxies form.

The disk of the Milky Way was first found to possess a *second* component with a larger scale height by Gilmore & Reid (1983). This component, which is known as the *thick disk*, contains more metal-poor and older stars than the thin disk. Thick disk stars are not only chemical, but also kinematically distinct from the thin disk population: a larger velocity ellipsoid, and an average galactic rotation velocity that lags the thin disk by some 30–40 km s $^{-1}$, as illustrates Fig. 8 (see also Gratton et al. 1996; Fuhrmann 1998; Bensby et al. 2005; Mishenina et al. 2004; Reddy et al. 2003). A recent study that exploits calibration stars observed as part of the Sloan Digital Sky Survey (SDSS) suggests that the peak of the metallicity distribution of the thick disk is always at $[\text{Fe}/\text{H}] \sim -0.7$ between 4 and 14 kpc from the galactic center (Allende Prieto et al. 2006), while local thick disk members selected based on kinematics indicate a high chemical homogeneity in this population (Reddy, Lambert & Allende Prieto 2006). These and other observations seem consistent with the thick disk emerging in a period of intensive accretion of smaller gas-rich galaxies by the Milky Way at a redshift > 1 or, equivalently, more than 8×10^9 yr ago (Brook et al. 2005).

Some of the oldest stars in the Milky Way have extremely low metal abundances, much lower than any globular cluster in the Galaxy. Their compositions may resemble that of the early Galaxy, with Li/H ratios similar to the proportions produced in the big bang. This, in fact, was the interpretation given by Spite & Spite (1982) to the nearly constant values of Li/H found in the surface of turn-off field stars with very low metal abundances. Experts still debate whether or not the Li abundance is exactly the same in the most metal-poor turn-off stars (e.g., Ryan et al. 1999, Meléndez & Ramírez 2004), but for our purposes it suffices to say that big bang nucleosynthesis models yield different

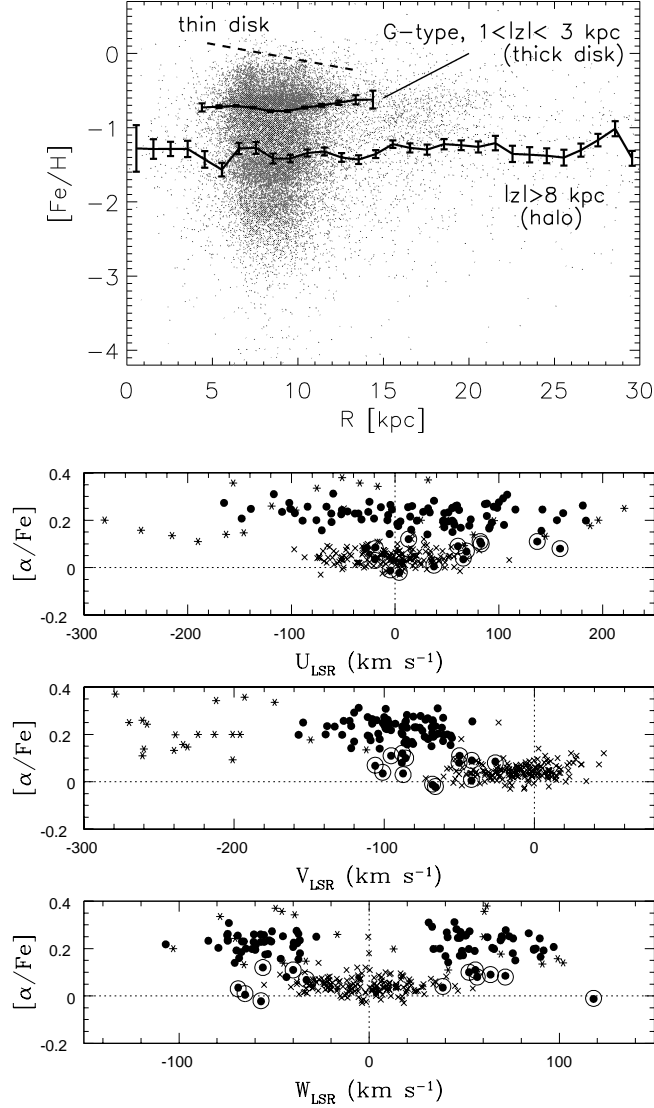


Figure 8. Top panel: some 20,000 F- and G-type stars with $14 < V < 20$ mag spectroscopically observed as part of the SDSS are used here to trace the median metallicity of the thick disk and the halo as a function of distance from the Galactic center (R in cylindrical coordinates). In this figure z is the distance from the galactic plane. The flat values of the median iron abundances contrast with the gradients reported in the literature for the thin disk (the dash line shows the mean metal abundances derived for B-type stars by Daflon & Cunha 2004). Adapted from Allende Prieto et al. (2006). Bottom panels: Chemical and kinematical separation of thick disk (filled circles), thin disk (crosses), and halo (asterisks) stars – plus the enigmatic stars with thick-disk kinematics and thin-disk abundances (filled circles surrounded by open circles). Here α indicates an average of Mg, Si, Ca and Ti. Adapted from Reddy et al. (2006).

Li/H ratios depending on the universe’s photon to baryon ratio, and therefore the lithium abundances in stars can constrain such an important cosmological parameter.

When old very metal-poor halo stars formed, there were very few metals around to be incorporated in the stars’ atmospheres. As massive stars die exploding as Type II supernovae, there must have been a period of high chemical heterogeneity in the halo. If a star happened to form at such early stages near the location where a supernova exploded, it could pick up the proportions of heavy elements produced before and during the explosion. That may have been the case for CS 22892-052, an extremely metal-poor ($[\text{Fe}/\text{H}] = -3.1$) and old (age $> 11 \times 10^9$ yr) halo giant which is highly enriched in neutron-capture elements (Snedden et al. 1994, 2003), and also for several other well-known cases, such as BD +17 3248 (Cowan et al. 2002), or HD 115444 (Westin et al. 2000). As Fig. 9 illustrates, the abundance patterns of heavy neutron-capture elements in these stars are remarkably similar to the *r*-process contribution to the solar-system abundances of these elements (as inferred by two different methods: Burris et al. 2000 vs. Arlandini et al. 1999). The *r*-process nucleosynthesis operates when high neutron fluxes are available, and it is usually associated with Type II supernovae. Therefore measuring abundances in these stars allows us to study supernova yields. Ongoing active searches for more of these interesting objects are already producing results (Barklem et al. 2005).

3.2. If the golden rule does not apply

The chemical composition of the atmosphere of a star may have changed since the star formed. As research has already shown, this can happen by a myriad of different processes. An interesting example of the use of stellar abundances under these circumstances is very close to home. Chemical abundances derived for the solar photosphere have been found to provide valuable clues on the structure of the solar interior. Considering diffusion in the solar convection zone is necessary to match the p-mode frequencies from helioseismic observations (e.g., Demarque & Guenther 1988, Christensen-Dalsgaard 2002, Lodders 2003). Since the formation of the Sun 4.57×10^9 years ago, the surface abundance of He relative to H has seen a reduction of 18 %, while the abundances of heavier elements have been reduced by 16 %.

The surface abundances of Li or Be in late-type stars can change significantly when the material is transported by convection to more interior zones where the temperature reaches a few million degrees and these light nuclei are destroyed. This violation of the golden rule has been exploited to learn about stellar structure by studying abundances in clusters (e.g. Boesgaard et al. 2004, García López, Rebolo & Pérez de Taoro 1995).

We discussed above how supernova yields can be inferred from rare metal-poor stars when the golden rule applies, but some have also attempted to do the same when the rule is not respected. Binary systems that have as a primary a neutron star or a black hole offer a chance to detect supernova ejecta that may have been blocked by the companion. González-Hernández et al. (2005) detected unusual enhancements of Ti and Ni ratios in the K-type companion of the neutron star Cen X-4, and concluded by comparison with theoretical calculations that the observed abundances could be explained by a spherically symmetric

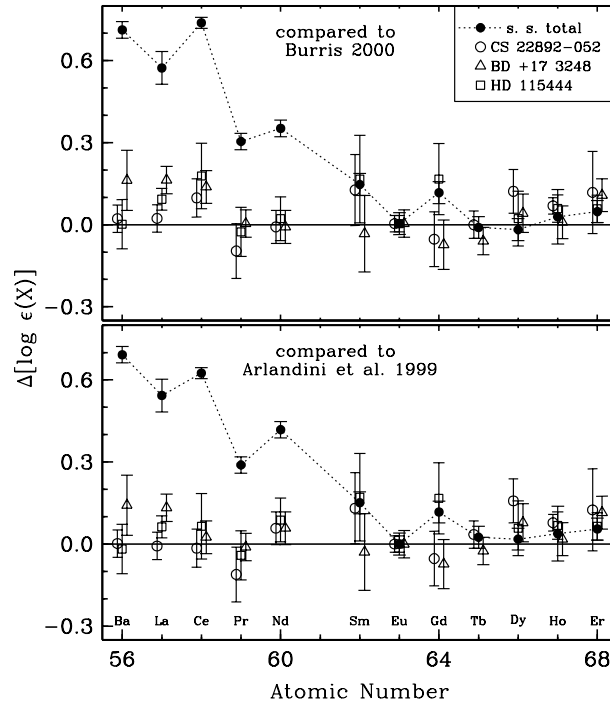


Figure 9. Differences between the abundances of heavy neutron capture elements in three stars and the *r-process* component of the solar abundances. The *r-process* solar abundances were inferred by subtracting the *s-process* (slow neutron capture) abundances estimated by two different methods: an empirical approach (Burris et al. 2000) or AGB stars nucleosynthesis models (Arlandini et al. 1999). The patterns have been normalized to force a perfect agreement for europium. Adapted from Lawler et al. (2005).

supernova explosion. Nevertheless, the kinematics of the system supports an asymmetric supernova, leaving open an interesting puzzle.

Perhaps one of the worse cases of the golden rule being broken is that of the RV Tauri variables. The photospheres of these stars exhibit dramatic abundance anomalies that correlate with condensation temperature (T_c). Elements with a high T_c can be depleted by several orders of magnitude respect to those with a low T_c . The elements depleted form dust grains, ending up in some sort of circumstellar reservoir, or being driven away by a stellar wind. Fig. 10 shows the abundance pattern derived for UY Cam by Giridhar et al. (2005). Metal-deficient post-AGB stars such as HR 4049 (Van Winckel, Waelkens & Waters 1995) exhibit a photospheric iron abundance $[\text{Fe}/\text{H}] \simeq -5.0$ but most likely started up with a near-solar Fe/H ratio. HR 4049 and its class seem to be all members of binary systems, and the same could be true for RV Tauris. We refer the reader to the recent review by Van Winckel (2003) for more on the amazing fauna of post-AGB stars.

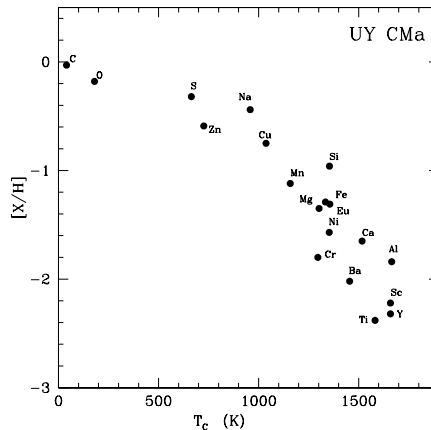


Figure 10. Abundance pattern in the RV Tauri star UY CMa. There is a strong correlation of the abundances with the condensation temperature. Adapted from Giridhar et al. (2005).

4. Conclusions

Recent noteworthy trends in research on stellar abundances include the development of improved model atmospheres for solar-like stars considering hydrodynamics, the availability of full-NLTE line-blanketed model atmospheres for hot stars, significant improvements in the opacities and the treatment of clouds for the coolest stars and brown dwarfs, the emergence of large spectroscopic surveys producing public data bases (e.g., SDSS, Elodie, S⁴N, SEGUE, GALEX), significant progress toward the automation of spectroscopic analyses, and in availability of accurate atomic data for neutron-capture elements.

A desirable short-term future would include 3D model atmospheres for late-type stars of all types, 1D models in full NLTE, NLTE line formation in 3D models, solar atlases observed at different positions on the disk to test line formation and model atmospheres, stronger efforts to measure/compute the necessary atomic and molecular data, stronger efforts to use the newly available atomic and molecular data, full analysis automation, a new generation of all-in-one archives (or virtual observatories) for both multi-wavelength observations and models, and ultra-high resolution spectrographs on large telescopes. Let's make it happen!

Acknowledgments. I am thankful to the organizers for a delightful meeting, and the opportunity to think (loud) about the field of stellar abundance determination. Some of the figures in this paper were kindly provided by A. Burrows, S. Giridhar, I. Hubeny, T. Lanz, J. Lawler, B. Reddy, and C. Sneden. The Swedish 1-m Solar Telescope is operated on the island of La Palma by the Institute for Solar Physics of the Royal Swedish Academy of Sciences in the Spanish Observatorio del Roque de los Muchachos of the Instituto de Astrofísica de Canarias. Support from NASA (NAG5-13057, NAG5-13147) is gratefully acknowledged.

References

- Allard, F., Hauschildt, P. H., Alexander, D. R., & Starrfield, S. 1997, *ARA&A*, 35, 137
- Allende Prieto, C. 2003, *MNRAS*, 339, 1111
- Allende Prieto, C., Asplund, M., García López, R. J., & Lambert, D. L. 2002, *ApJ*, 567, 544
- Allende Prieto, C., Beers, T. C., Wilhelm, R., Newberg, H. J., Rockosi, C. M., Yanny, B., & Lee, Y. S. 2006, *ApJ*, 636, 804
- Allende Prieto, C., Lambert, D. L., & Asplund, M. 2001, *ApJ*, 556, L63
- Allende Prieto, C., Lambert, D. L., & Asplund, M. 2002, *ApJ*, 573, L137
- Allende Prieto, C., Lambert, D. L., Hubeny, I., & Lanz, T. 2003a, *ApJS*, 147, 363
- Allende Prieto, C., Hubeny, I., & Lambert, D. L. 2003b, *ApJ*, 591, 1192
- Antia, H. M., & Basu, S. 2005, *ApJ*, 620, L129
- Arlandini, C., Käppeler, F., Wisshak, K., Gallino, R., Lugaro, M., Busso, M., & Straniero, O. 1999, *ApJ*, 525, 886
- Asplund, M. 2005, *ARA&A*, 43, 481
- Asplund, M., Grevesse, N., Sauval, A. J., Allende Prieto, C., & Kiselman, D. 2004, *A&A*, 417, 751
- Asplund, M., Grevesse, N., Sauval, A. J., Allende Prieto, C., & Blomme, R. 2005, *A&A*, 431, 693
- Asplund, M., Nordlund, Å., Trampedach, R., Allende Prieto, C., & Stein, R. F. 2000a, *A&A*, 359, 729
- Asplund, M., Nordlund, Å., Trampedach, R., & Stein, R. F. 2000b, *A&A*, 359, 743
- Bahcall, J. N., Basu, S., Pinsonneault, M., & Serenelli, A. M. 2005a, *ApJ*, 618, 1049
- Bahcall, J. N., Basu, S., & Serenelli, A. M. 2005b, *ApJ*, 631, 1281
- Bahcall, J. N., Serenelli, A. M., & Basu, S. 2005c, *ApJ*, 621, L85
- Barklem, P. S., Anstee, S. D., & O'Mara, B. J. 1998, *PASA*, 15, 336
- Barklem, P. S., & Asplund-Johansson, J. 2005, *A&A*, 435, 373
- Barklem, P. S., et al. 2005, *A&A*, 439, 129
- Barklem, P. S., Piskunov, N., & O'Mara, B. J. 2000, *A&A*, 363, 1091
- Barklem, P. S., Stempels, H. C., Allende Prieto, C., Kochukhov, O. P., Piskunov, N., & O'Mara, B. J. 2002, *A&A*, 385, 951
- Basu, S., & Antia, H. M. 2004, *ApJ*, 606, L85
- Basu, S., Pinsonneault, M. H., & Bahcall, J. N. 2000, *ApJ*, 529, 1084
- Bensby, T., Feltzing, S., Lundström, I., & Ilyin, I. 2005, *A&A*, 433, 185
- Boesgaard, A. M., Armengaud, E., King, J. R., Deliyannis, C. P., & Stephens, A. 2004, *ApJ*, 613, 1202
- Brook, C. B., Veilleux, V., Kawata, D., Martel, H., & Gibson, B. K. 2005b, *Proceedings of "Island Universes: Structure and Evolution of Disk Galaxies"* (astro-ph/0511002)
- Böhm-Vitense, E. 1958, *Zeitschrift für Astrophysics*, 46, 108
- Burris, D. L., Pilachowski, C. A., Armandroff, T. E., Sneden, C., Cowan, J. J., & Roe, H. 2000, *ApJ*, 544, 302
- Burrows, A., et al. 1997, *ApJ*, 491, 856
- Burrows, A., Sudarsky, D., & Hubeny, I. 2005, *ApJ*, submitted (astro-ph/0509066)
- Christensen-Dalsgaard, J. 2002, *Reviews of Modern Physics*, 74, 1073
- Cowan, J. J., et al. 2002, *ApJ*, 572, 861
- Cowley, C. R., & Bautista, M. 2003, *MNRAS*, 341, 1226
- Dafon, S., & Cunha, K. 2004, *ApJ*, 617, 1115
- Demarque, P., & Guenther, D. B. 1988, *IAU Symp. 123: Advances in Helio- and Asteroseismology*, 123, 91
- Den Hartog, E. A., Herd, M. T., Lawler, J. E., Sneden, C., Cowan, J. J., & Beers, T. C. 2005, *ApJ*, 619, 639
- Den Hartog, E. A., Wickliffe, M. E., & Lawler, J. E. 2002, *ApJS*, 141, 255
- Drake, J. J., & Testa, P. 2005, *Nature*, 436, 525

- Erspamer, D., & North, P. 2003, *A&A*, 398, 1121
- Fuhrmann, K. 1998, *A&A*, 338, 161
- García López, R. J., Rebolo, R., & Pérez de Taoro, M. R. 1995, *A&A*, 302, 184
- Gilmore, G., & Reid, N. 1983, *MNRAS*, 202, 1025
- Giridhar, S., Lambert, D. L., Reddy, B. E., Gonzalez, G., & Yong, D. 2005, *ApJ*, 627, 432
- González Hernández, J. I., Rebolo, R., Israelian, G., Casares, J., Maeda, K., Bonifacio, P., & Molaro, P. 2005, *ApJ*, 630, 495
- Gratton, R., Carretta, E., Matteucci, F., & Sneden, C. 1996, *ASP Conf. Ser.* 92: Formation of the Galactic Halo, H. L. Morrison and A. Sarajedini, eds., 92, 307
- Gustafsson, B., Bell, R. A., Eriksson, K., & Nordlund, Å. 1975, *A&A*, 42, 407
- Gustafsson, B., Edvardsson, B., Eriksson, K., Mizuno-Wiedner, M., Jørgensen, U. G., & Plez, B. 2003, *ASP Conf. Ser.* 288: Stellar Atmosphere Modeling, 288, 331
- Gustafsson, B., & Jørgensen, U. G. 1994, *A&A Rev.*, 6, 19
- Hillier, D. J. 2003, *ASP Conf. Ser.* 288: Stellar Atmosphere Modeling, 288, 199
- Hubeny, I., & Lanz, T. 1995, *ApJ*, 439, 875
- Hurlburt, N. E., Toomre, J., & Massaguer, J. M. 1984, *ApJ*, 282, 557
- Katz, D., Soubiran, C., Cayrel, R., Adda, M., & Cautain, R. 1998, *A&A*, 338, 151
- Kirkpatrick, J. D. 2005, *ARA&A*, 43, 195
- Kurucz, R. 1993, CD-ROM No. 15. Cambridge, Mass.: SAO
- Lanz, T., & Hubeny, I. 2003, *ApJS*, 146, 417
- Lawler, J. E., Sneden, C., & Cowan, J. J. 2004, *ApJ*, 604, 850
- Lawler, J. E., Wyart, J.-F., & Blaise, J. 2001, *ApJS*, 137, 351
- Lodders, K. 2003, *ApJ*, 591, 1220
- Massaguer, J. M., & Zahn, J.-P. 1980, *A&A*, 87, 315
- Mishenina, T.V., Soubiran, C., Kovtyukh, V.V., & Korotin, S.A. 2004, *A&A*, 418, 551
- Montalbán, J., Miglio, A., Noels, A., Grevesse, N., & di Mauro, M. P. 2004, *ESA SP-559: SOHO 14 Helio- and Asteroseismology: Towards a Golden Future*, 14, 574
- Meléndez, J., & Ramírez, I. 2004, *ApJ*, 615, L33
- Nahar, S. N., & Pradhan, A. K. 2005, *A&A*, 437, 345
- Nordlund, Å. 1980, *Lecture Notes in Physics*, Berlin Springer Verlag, 114, 213
- Pauldrach, A. W. A., Hoffmann, T. L., Lennon, M. 2001, *A&A*, 375, 161
- Piskunov, N. E., & Valenti, J. A. 2002, *A&A*, 385, 1095
- Rauch, T. 2003, *A&A*, 403, 709
- Ryan, S. G., Norris, J. E., & Beers, T. C. 1999, *ApJ*, 523, 654
- Reddy, B.E., Tomkin, J., Lambert, D.L., & Allende Prieto, C. 2003, *MNRAS*, 340, 304
- Reddy, B.E., Lambert, D.L., & Allende Prieto, C. 2006, *MNRAS*, in press
- Repolust, T., Puls, J., & Herrero, A. 2004, *A&A*, 415, 349
- Ritter, A., & Washuettl, A. 2004, *Astronomische Nachrichten*, 325, 663
- Robinson, F. J., Demarque, P., Li, L. H., Sofia, S., Kim, Y.-C., Chan, K. L., & Guenther, D. B. 2004, *MNRAS*, 347, 1208
- Seaton, M. J. 2005, *MNRAS*, 362, L1
- Short, C. I., & Hauschildt, P. H. 2005, *ApJ*, 618, 926
- Sneden, C., Preston, G. W., McWilliam, A., & Searle, L. 1994, *ApJ*, 431, L27
- Sneden, C., et al. 2003, *ApJ*, 591, 936
- Snider, S., Allende Prieto, C., von Hippel, T., Beers, T. C., Sneden, C., Qu, Y., & Rossi, S. 2001, *ApJ*, 562, 528
- Spite, F., & Spite, M. 1982, *A&A*, 115, 357
- Stein, R. F., & Nordlund, Å. 1998, *ApJ*, 499, 914
- Tsuji, T. 2005, *ApJ*, 621, 1033
- Van Winckel, H. 2003, *ARA&A*, 41, 391
- Van Winckel, H., Waelkens, C., & Waters, L. B. F. M. 1995, *A&A*, 293, L25
- Westin, J., Sneden, C., Gustafsson, B., & Cowan, J. J. 2000, *ApJ*, 530, 783
- Willemssen, P. G., Hilker, M., Kayser, A., & Bailer-Jones, C. A. L. 2005, *A&A*, 436, 379
- Young, P. A., & Arnett, D. 2005, *ApJ*, 618, 908